

# The crystal growth and thermoelectric properties of chromium disilicide

I. NISHIDA

National Research Institute for Metals, Meguro-ku, Tokyo, Japan

Single crystals of chromium disilicide about 8 mm in diameter and 35 mm long were grown using the floating zone technique. Measurements of electrical resistivity  $\rho$ , Hall coefficient  $R$  and thermoelectric power  $\alpha$  were carried out in the temperature range from 85 to 1100 K. The values of  $\rho$  and  $\alpha$  showed the anisotropy over the temperature range studied. The ratios parallel and perpendicular to the  $c$ -axis were  $\rho_{\parallel}/\rho_{\perp} = 1.9$  and  $\alpha_{\parallel}/\alpha_{\perp} = 1.7$  respectively, at room temperature. It was found to be a degenerate semiconductor having the hole concentration of  $6.3 \times 10^{20} \text{ cm}^{-3}$  below 600 K. The effective masses of holes parallel and perpendicular to the  $c$ -axis determined from the thermoelectric power and the hole concentration near room temperature were estimated to be five and three times as large as a free electron mass, respectively. The calculation on the values of  $\alpha_{\parallel}$  and  $\alpha_{\perp}$  was made using those effective masses. These values showed good agreement with the observed values in the temperature range from 150 to 1100 K.

## 1. Introduction

The thermoelectric properties of 3d-transition metal silicides have been reported by many investigators [1-12]. In particular, the chromium, manganese and iron disilicides have been well known as compounds having semiconducting properties [8-12]. On the other hand, these silicides are interesting materials as thermoelectric conversion elements which can be utilized for generating electric power at high temperature [9, 13, 14]. In recent years, thermomaterials composed of a chromium disilicide and a cobalt monosilicide have been applied as the electric sources for hot air circulators and magnetic safety valves for gas stoves [14]. However, since it was difficult to make a large single crystal of chromium disilicide, the previous investigations were mainly carried out on polycrystalline specimens. Also, since the crystal structure of chromium disilicide belongs to a space group  $D_6^4$  having lattice parameters of  $a = 4.422 \pm 0.005 \text{ \AA}$ ,  $c = 6.351 \pm 0.005 \text{ \AA}$  and  $c/a = 1.44$  [15], the thermoelectric properties of the crystals should be anisotropic with differing values parallel and perpendicular to  $c$ -axis direction. The thermoelectric properties for the chromium disilicide crystals grown using the Czochralski method have been reported by Shinoda *et al* [16]

and Voronov *et al* [17]. However, no detailed investigations for the crystal growth and the anisotropy of thermoelectric properties were carried out.

The purpose of the present study was not only to investigate the crystal growing procedure and to examine the anisotropy of the thermoelectric properties for single crystal of chromium disilicide, but also to calculate the temperature dependence of the thermoelectric powers parallel and perpendicular to the  $c$ -axis direction based on the assumptions that the top of the valence band is parabolic and that the carriers obey Fermi-Dirac statistics.

## 2. Crystal growth of chromium disilicide

The chromium monosilicide powder was prepared from chromium (purity of 99.9%) containing 50 at. % silicon (purity of 99.9%) by a solid-state reaction in a sealed quartz tube at temperature of 800 to 1000°C. The chromium monosilicide was identified by X-ray analysis and was ground into a fine powder of a few microns. The powder was hot-pressed into a size 6 mm square by 80 mm in an argon atmosphere at 1250°C for 8 min under a pressure of about 300 kg cm<sup>-2</sup> and was refined to obtain the high purity silicide by floating zone melting using a

refining speed of 3 mm per min in an argon atmosphere containing 10 vol % hydrogen. By repeating a few operations of zone refining, the square specimen was completely changed into a rod and was crystallized into many small crystals with an average size of  $9 \text{ mm}^3$ . Individual crystals in the coarse-grained rod were used for chromium disilicide as the matrix alloy. The apparatus used for crystal growth of chromium disilicide is illustrated in Fig. 1. The apparatus is generally utilized for refining materials, but it has undergone various improvements using the carbon holder with a conical hole which can be set up on the rotor shaft as the after heater. Consequently, the specimen contained in the conical quartz crucible is heated by the induction coil and rotated with the carbon holder and the rotor shaft to produce homogeneous heating.

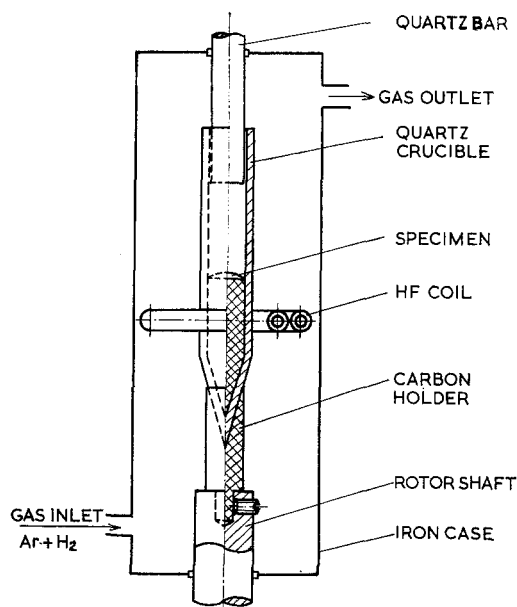


Figure 1 Schematic diagram of the apparatus used for crystal growth.

A chromium disilicide ingot was prepared by melting the mixture of the chromium monosilicide crystal adding the high purity single crystal silicon (purity of 99.999% with *n*-type semiconduction) in an argon atmosphere. The ingot was so porous and very brittle that it was easily crushed down to a size of about  $3 \text{ mm}^3$ , and the individual crystals were transferred to a transparent conical quartz crucible. They were repeatedly melted with the induction coil to obtain a large single crystal using a refining speed

of 0.17 to 3 mm per min in an argon atmosphere containing 10 vol % hydrogen at about  $1550^\circ\text{C}$ . The single crystal of chromium disilicide was grown into a size of about 8 mm in diameter and 35 mm long.

The single crystal of chromium disilicide confirmed that its growth direction is approximately parallel to the *c*-axis and the lattice parameters are:  $a = 4.424\text{\AA}$ ,  $c = 6.347\text{\AA}$  and  $c/a = 1.44$ . These are in good agreement with those reported previously [15, 18], and also the chemical composition was chromium 33.58 at. % and silicon of 66.42 at. % ( $\pm 0.01$ ).

### 3. Experimental procedure

In order to measure the thermoelectric properties for single crystals of chromium disilicide, the specimens were cut from a single crystal rod into rectangular parallelepiped form of about  $0.1 \times 4 \times 8 \text{ mm}$  by the diamond wheel so that its longitudinal direction was parallel to  $\langle 0001 \rangle$  or  $\langle 10\bar{1}0 \rangle$  direction. They were heated in a sealed quartz tube at about  $1100^\circ\text{C}$  for 200 h and cooled in the furnace. From the chemical analysis of the annealed specimens, the chemical compositions were determined to be chromium 33.57 at. % and silicon 66.43 at. % ( $\pm 0.01$ ). The compositions showed good agreement with as-grown single crystals.

An ordinary dc method [19] was used for measuring electrical resistivity and the Hall coefficient in an applied magnetic field from 500 to 6500 gauss. The method described by Sakata [5] was used for measurement of the thermoelectric power in an argon atmosphere at 100 mm Hg pressure in the temperature range 85 to 1100 K. The temperature difference between both ends of a specimen was maintained in the range of  $0.5$  to  $3.0^\circ\text{C}$ . The thermoelectromotive forces were measured with two potentiometers and the values of the thermoelectric power were obtained from the slopes of temperature versus thermoelectromotive force. The thermoelectric powers were calculated and absolute values derived.

### 4. Experimental results and discussions

#### 4.1. Anisotropy of thermoelectric properties

Fig. 2 shows the electrical resistivity  $\rho$  as a function of the reciprocal absolute temperature for the chromium disilicide. Both curves of resistivities  $\rho_{\parallel}$ ,  $\rho_{\perp}$  parallel and perpendicular to the *c*-axis show a similar variation, but the values of  $\rho_{\parallel}$  are larger than that of  $\rho_{\perp}$  over the whole

temperature range. The ratios of resistivities  $\rho_{\parallel}/\rho_{\perp}$  parallel and perpendicular to the  $c$ -axis show a nearly constant value of 1.9 below 700 K.

However, this value decreases with increasing temperature at higher temperatures. It can be seen that the changes in  $\rho_{\parallel}$  and  $\rho_{\perp}$  are described as a relationship of  $\rho \propto T^{-1}$  at high temperature. The forbidden energy gap  $E_g$  obtained from the temperature dependence of  $\rho$  is estimated to be  $E_g = 0.32$  eV. Using this value, the resistivities in the intrinsic region are expressed by  $\rho_{\parallel} = 3.0 \times 10^{-4} \exp(1850/T)$  and  $\rho_{\perp} = 1.6 \times 10^{-4} \exp(1850/T)$  ohm cm, respectively.

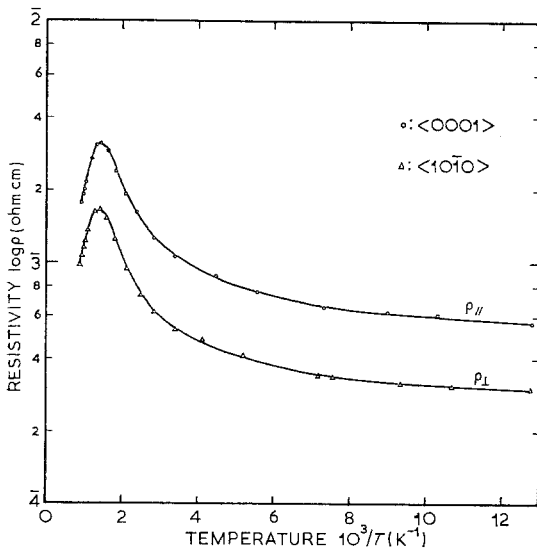


Figure 2 Electrical resistivity of the chromium disilicide crystals as a function of the reciprocal absolute temperature;  $\parallel$  is parallel,  $\perp$  is perpendicular to the  $c$ -axis.

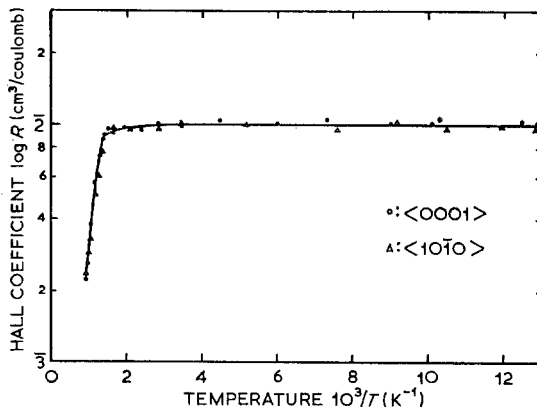


Figure 3 The variation of Hall coefficient with the reciprocal absolute temperature for the chromium disilicide crystals.

Fig. 3 shows the variation of the Hall coefficient with the reciprocal absolute temperature. The Hall coefficient  $R$  is independent of temperature below 600 K, and its sign is positive in the temperature range from 85 to 1100 K. In this experiment, no anisotropy of  $R$  is apparent and no magnetic dependence of  $R$  should be noted in the range of the magnetic field from 500 to 6500 gauss. Therefore, the chromium disilicide crystal could be recognized as a degenerate semiconductor having a hole concentration of  $6.2 \times 10^{20} \text{ cm}^{-3}$  below 600 K. A calculation of hole concentration for stoichiometric chromium disilicide was carried out based on an assumption that excess chromium atoms would act as acceptors in the crystal. The concentration of holes is estimated to be  $3.92 \times 10^{20} \text{ cm}^{-3}$  in reasonable agreement with that reported previously [16].

The temperature dependence of Hall mobility  $\mu = R/\rho$  is shown in Fig. 4. The Hall mobility  $\mu$  decreases with increasing temperature and the change is remarkably large above room temperature. At higher temperatures since the  $\mu$  is proportional to  $T^{-3/2}$ , acoustic lattice scattering of the carriers is considered to be dominant. A ratio of the mobilities  $\mu_{\parallel}/\mu_{\perp}$  parallel and perpendicular to  $c$ -axis has a constant value of 0.5 in the temperature range from 85 to 1100 K. The value of  $\mu_{\parallel}/\mu_{\perp} = 0.5$  is smaller than that obtained by Voronov [17], but this is considered to be more reasonable from the relationship between the Hall coefficient and resistivity because the Hall coefficient represents no anisotropy and  $\rho_{\parallel}/\rho_{\perp}$  is about 1.9. The hole mobilities  $\mu_{p\parallel}$ ,  $\mu_{p\perp}$  parallel and perpendicular to the  $c$ -axis obtained from the relationship between  $\rho$  and  $R$  data in the extrinsic region above 300 K are expressed by  $\mu_{p\parallel} = 4.8 \times 10^4 T^{-3/2}$  and  $\mu_{p\perp} = 9.4 \times 10^4 T^{-3/2} \text{ cm}^2 \text{ V}^{-1}$ , respectively.

Fig. 5 shows the thermoelectric power difference  $\Delta\alpha = \alpha_{\parallel} - \alpha_{\perp}$  between the parallel and perpendicular to the  $c$ -axis as a function of temperature. The thermoelectric power difference  $\Delta\alpha$  increases with increasing temperature and shows a maximum value at about 800 K. The changes of  $\Delta\alpha$  are very similar to the previously reported data, but the values are about 30% smaller than those reported previously [17]. Since the value of  $\Delta\alpha$  have large positive values in all temperature ranges, it can be seen that the effective masses of hole would be different between the directions parallel and perpendicular to the  $c$ -axis.

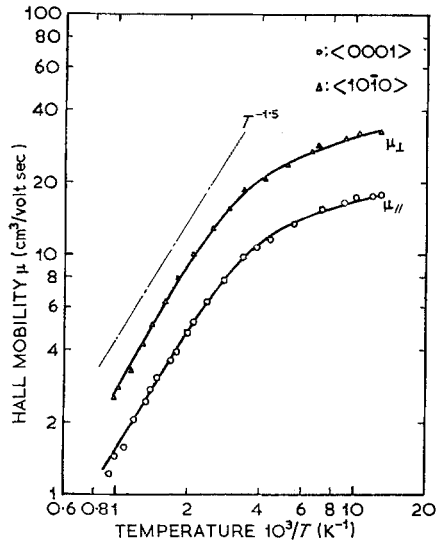


Figure 4 The temperature dependence of Hall mobility for the chromium disilicide crystals.

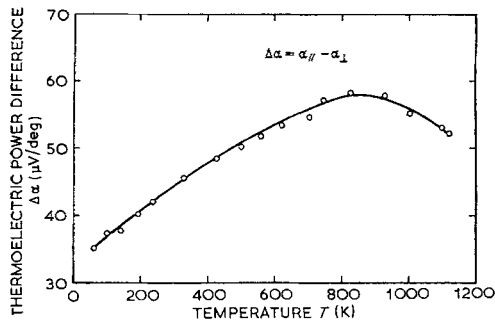


Figure 5 The thermoelectric power difference  $\Delta\alpha = \alpha_{||} - \alpha_{\perp}$  parallel and perpendicular to the  $c$ -axis for a chromium disilicide crystal.

#### 4.2. Analysis of thermoelectric powers

The temperature dependencies of thermoelectric powers  $\alpha_{||}$ ,  $\alpha_{\perp}$  parallel and perpendicular to the  $c$ -axis are shown in Fig. 6. The curves of the temperature dependencies of  $\alpha_{||}$  and  $\alpha_{\perp}$  show a similar variation, but the value of  $\alpha_{||}$  is relatively larger than that of  $\alpha_{\perp}$  in the whole temperature range. Maximum values obtained in  $\alpha_{||}$  and  $\alpha_{\perp}$  can be seen at about 700 K which is in agreement with those obtained in  $\rho$  data. Since the parameters have large positive values at the higher temperatures and the hole mobility  $\mu_p$  varies with  $T^{-3/2}$  (seen in Fig. 3), it is suggested that the ratio of electron mobility  $\mu_e$  to hole mobility  $\mu_p$  is probably smaller than unity. The calculation of  $\alpha$  was carried out based on the assumptions

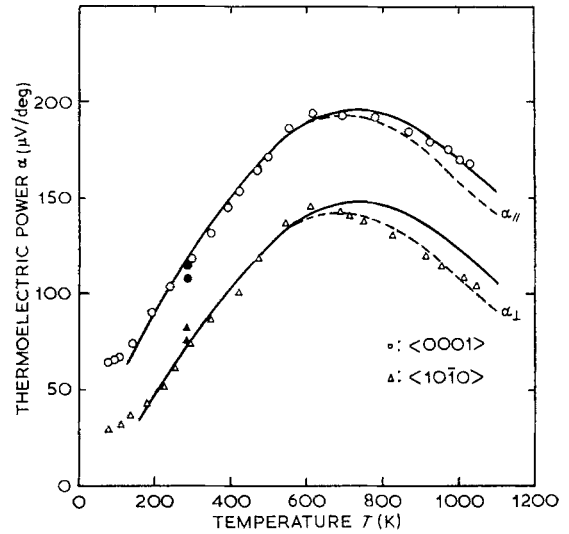


Figure 6 The temperature dependence of thermoelectric power for the chromium disilicide crystals. The solid curves represent the values calculated by using  $b = 0$  and the dotted curves the values calculated by using  $b = 0.01$ , and also the solid circles are data by Voronov.

that the top of valence band is parabolic, that the scattering of carriers is dominated by acoustic lattice scattering, and that the carriers obey Fermi-Dirac statistics. Thus the temperature dependence of hole concentration  $p$  and  $\alpha$  are given by the following equations [20].

$$p = \frac{4\pi(2m_p^* kT)^{3/2}}{h^3} F_{1/2}(\eta_p^*) \quad (1)$$

$$\alpha = \pm \frac{k}{e} \left\{ 2 \frac{F_1(\eta^*)}{F_0(\eta^*)} - \eta^* \right\}, \quad (2)$$

where  $m_p^*$  is the effective mass of a hole,  $\eta^*$  is either the reduced Fermi energy of holes or of electrons and  $\eta_p^*$  corresponds to holes,  $k$  is Boltzmann's constant,  $e$  is an electron charge, and  $F_r(\eta^*)$  is a well-known function called Fermi-dirac integral and is expressed by

$$F_r(\eta^*) = \int_0^\infty \frac{\epsilon^r d\epsilon}{\exp\left(\frac{\epsilon}{kT} - \eta^*\right) + 1} \quad (3)$$

The + and - signs correspond to holes and electrons, respectively.

To calculate the temperature dependence of  $\alpha_{||}$  and  $\alpha_{\perp}$  for the chromium disilicide crystal, the effective masses of hole  $m_{p||}^*$ ,  $m_{p\perp}^*$  parallel and perpendicular to the  $c$ -axis were estimated from the data of the thermoelectric power and Hall

coefficient using Equations 1 and 2 near room temperature. This gives  $m_{p\parallel}^*$  and  $m_{p\perp}^*$  as five and three times as large as a free electron mass  $m_0$ , respectively. Assuming that these values are independent of temperature and that the hole concentration is constant, the values of  $\eta_p^*$  at various temperatures are estimated from Equation 1, and these are then used in Equation 2 to calculate the temperature dependence of  $\alpha_{\parallel}$  and  $\alpha_{\perp}$ . The calculated values of  $\alpha_{\parallel}$  and  $\alpha_{\perp}$  are in reasonable agreement with those observed over the temperature range from 150 to 600 K.

On the other hand, when both holes and electrons are present  $\alpha$  is given by

$$\alpha = \rho \{ (\alpha_p / \rho_p) + (\alpha_e / \rho_e) \}, \quad (4)$$

where  $\alpha_p$  and  $\alpha_e$  are the partial thermoelectric powers of holes and electrons respectively, and  $\rho_p$  and  $\rho_e$  are the resistivities corresponding to holes and electrons, respectively. Using the relation of  $\eta_p^* + \eta_e^* = -\xi^*$ , where  $\eta_e^*$  is the reduced Fermi energy for holes and  $\xi^*$  is an energy gap in unit of  $kT$ , Equation 4 is expressed by

$$\alpha = \frac{k}{e(nb + p)} \left[ 2p \frac{F_1(\eta_p^*)}{F_0(\eta_p^*)} - nb \left\{ 2 \frac{F_1(-\eta_p^* - \xi^*)}{F_0(-\eta_p^* - \xi^*)} + \xi_p^* \right\} - \eta_p^*(nb + p) \right]. \quad (5)$$

In the temperature range higher than 600 K, two equations as described by Pearson [21] were used in the analysis of the hole concentration  $p$  and the electron concentration  $n$ . The equations for  $p$ -type semiconductor are given by

$$p = \left( \frac{1}{e\rho\mu_p} + bN_s \right) / (b + 1), \quad (6)$$

$$n = p - N_s, \quad (7)$$

where  $N_s$  is the hole concentration in the degenerate state. These results were used in the calculations of  $\alpha_{\parallel}$  and  $\alpha_{\perp}$  in the intrinsic region. Using both a constant value of  $m_{p\parallel}^* = 5m_0$  and the hole concentration obtained from the data of  $\rho_{\parallel}$  and  $\mu_{p\parallel}$  at the various temperatures, Equation 6, the values of  $\eta_p^*$  were estimated from Equation 1 and these were then used in Equation 5 to calculate the temperature dependence of  $\alpha_{\parallel}$ . Both the experimentally determined value of  $E_g = 0.32$  eV and an assumed value of  $b = 0$  were also used in the calculation (Shinoda has reported that the value of  $b$  is probably of the order of 0.01 or less [16]). In much the same way

as the calculation of  $\alpha_{\parallel}$ , the temperature dependence of  $\alpha_{\perp}$  was calculated from Equations 1, 5 and 6 using a value of  $m_{p\perp}^* = 3m_0$ . The results are shown as the solid curve in Fig. 6. These values are in reasonable agreement with the observed values of  $\alpha_{\parallel}$  in the temperature range from 150 to 1100 K. In the temperature range above 600 K, however, the calculated values of  $\alpha_{\perp}$  are not in agreement with the observed values.

The discrepancy between the calculated and the observed values in the temperature range higher than 600 K might have resulted from the calculations neglecting the contribution of the electron in the intrinsic region. In order to correct the discrepancy, the values of  $p$  and  $n$  were estimated from the data of  $\rho$ ,  $\mu_p$  and Hall coefficient in the various temperatures using a constant value of  $b = 0.01$  and Equations 6 and 7. Using these results and  $b = 0.01$ , the temperature dependences of  $\alpha_{\parallel}$  and  $\alpha_{\perp}$  were also calculated from the Equations 1 and 5. The experimentally determined values of  $m_{p\parallel}^* = 5m_0$  and  $m_{p\perp}^* = 3m_0$  at room temperature were used in the calculation. These results are shown as the dotted curve in Fig. 6. The values are in reasonable agreement with the observed  $\alpha_{\perp}$  over the temperature range from 150 to 1100 K, but the calculated values of  $\alpha_{\parallel}$  are smaller than that observed in the temperature range higher than 600 K. Accordingly, it is considered that the mobility ratio parallel to the  $c$ -axis for chromium disilicide is very much smaller than that perpendicular to the  $c$ -axis.

On the other hand, the relationship between  $m_p^*$  and  $\mu_p$  is described by  $\mu_p = m_p^{*-5/3}$  for acoustic lattice scattering [20], the hole mobility ratio of  $\mu_{p\parallel}$  to  $\mu_{p\perp}$  is given as:

$$\frac{\mu_{p\parallel}}{\mu_{p\perp}} = \left[ \frac{m_{p\perp}^*}{m_{p\parallel}^*} \right]^{5/3}. \quad (8)$$

Substitution of  $m_{p\parallel}^* = 5m_0$  and  $m_{p\perp}^* = 3m_0$  into Equation 8 gives  $\mu_{p\parallel}/\mu_{p\perp} = 0.45$ . This value fits approximately a value of 0.50 obtained from  $R$  and  $\rho$  data. From the calculated results, the hole effective masses parallel and perpendicular to  $c$ -axis are estimated to be  $5m_0$  and  $3m_0$ , respectively.

## 5. Conclusions

Single crystals of chromium disilicide were grown using the floating zone melting technique. The crystals produced were about 8 mm in diameter and 35 mm long and the grown direction was

approximately parallel to the  $c$ -axis. The chemical composition was chromium 33.58 at. % and silicon 66.42 at. %.

From the measurements of electrical resistivity  $\rho$ , Hall coefficient  $R$ , and thermoelectric power  $\alpha$  in the temperature range from 85 to 1100 K, it is found that  $\rho$  and  $\alpha$  have an anisotropy over the temperature range studied and that these ratios parallel and perpendicular to the  $c$ -axis are  $\rho_{\parallel}/\rho_{\perp} = 1.9$  and  $\alpha_{\parallel}/\alpha_{\perp} = 1.7$  at room temperature. Furthermore, it is found that the single crystals are a degenerate semiconductor having a hole concentration of about  $6.3 \times 10^{20} \text{ cm}^{-3}$  below 600 K, and that excess chromium atoms act as acceptors in the crystal. The intrinsic resistivities are  $\rho_{\parallel} = 3.0 \times 10^{-4} \exp(1850/T)$  and  $\rho_{\perp} = 1.6 \times 10^{-4} \exp(1850/T)$  ohm cm.

From the calculated results of  $\alpha$  and carrier concentration in the temperature range between 85 and 1100 K, it is estimated that the effective masses of hole  $m_{p_{\parallel}}^*$ ,  $m_{p_{\perp}}^*$  and the ratios of electron to hole mobility  $b_{\parallel}$ ,  $b_{\perp}$  parallel and perpendicular to  $c$ -axis are  $m_{p_{\parallel}}^* = 5m_0$ ,  $m_{p_{\perp}}^* = 3m_0$  and  $b_{\parallel} \ll b_{\perp} = 0.01$ , respectively. By assuming that the scattering of carriers is dominated by acoustic lattice scattering and that the effective masses is independent of the temperature, the calculated values of  $\alpha_{\parallel}$  and  $\alpha_{\perp}$  are in reasonable agreement with the observed values over the temperature range from 150 to 1100 K.

### Acknowledgement

The author would like to express thanks to Professor T. Sakata of Science University of Tokyo, for his kind guidance, and to Mrs K. Sakata of Metal Physics Division and Mr T. Tokushima of Nippon Gakki, for their co-operation.

### References

1. L. N. GUSEVA and B. N. OVECHKIN, *Doklady Akad. Nauk SSSR* **112** (1957) 681.

2. E. N. NIKITIN, *Zhur. Tekh. Fiz.* **28** (1958) 26.
3. Y. SASAKI, S. ASANABE, and D. SHINODA, *Phys. Soc. Japan Meeting*, April (1959) 68.
4. E. N. NIKITIN, *Soviet Physics-Solid State* **1** (1959) 304.
5. T. SAKATA and T. TOKUSHIMA, *Trans. Nat. Res. Inst. Metals (Japan)* **5** (1963) 34.
6. V. A. KORSHUNOV and P. V. GEL'D, *Fiz. Metal. i Metalloved.* **11** (1960) 945.
7. L. D. IVANOVA, N. KH. ABRIKOSOV, E. I. ELAGINA, and V. D. KHBOSTIKVA, *Neorg. Material* **5** (1969) 1933.
8. W. B. BIENERT and E. A. SKRABEK, *Proc. IEEE/AIAA Thermoelectric Specialists Conf.* **10** (1966) 1.
9. R. M. WARE and D. J. MCHIELL, *Proc. IEE*, **111** (1964) 178.
10. U. BIRKHOLZ and J. SCHELM, *Phys. Stat. Sol.* **27** (1968) 413.
11. J. HESSE, *Z. Metallk.* **60** (1969) 653.
12. U. BIRKHOLZ and A. FRUHAUE, *Phys. Stat. Sol.* **34** (1969) K177.
13. R. KIEFFER, F. BENESOVSKY, and C. KONPICKY, *Ber. deutsche keram. Ges.* **31** (1954) 223.
14. T. TOKUSHIMA, I. NISHIDA, K. SAKATA, and T. SAKATA, *J. Mater. Sci.* **4** (1969) 978.
15. B. BOREN, *Arkiv. Kem. Mineral Geol.* **11A** (1933) no. 10, 1.
16. D. SHINODA, S. ASANABE, and Y. SASAKI, *J. Phys. Soc. Japan* **19** (1964) 269.
17. B. K. VORONOV, L. D. DUDKIN, and N. N. TRUSOVA, *Kristallografiya* **12** (1967) 519.
18. L. P. ZELENIN, I. Z. RADOVSKII, F. A. SIDORENKO, P. V. GEL'D, and B. S. RABINOVICH, *Poriskobaya Met.* **2** (1966) 67.
19. E. H. PUTLEY, "The Hall Effect and Related Phenomena" (Butterworth Co. London, 1960) p. 61.
20. A. F. IOFFE, "Physics of Semiconductors" (Inforsearch Ltd, London, 1960) p. 305.
21. G. L. PEARSON and F. BARDEEN, *Phys. Rev.* **75** (1949) 865.

Received 6 and accepted 25 February 1972.